Phases of Aβ-deposition in the human brain and its relevance for the development of AD

Dietmar R. Thal, MD; Udo Rüb, MD; Mario Orantes, MD; and Heiko Braak, MD

Abstract—*Background:* The deposition of the amyloid β protein (Aβ) is a histopathologic hallmark of AD. The regions of the medial temporal lobe (MTL) are hierarchically involved in Aβ-deposition. *Objective:* To clarify whether there is a hierarchical involvement of the regions of the entire brain as well and whether there are differences in the expansion of Aβ-pathology between clinically proven AD cases and nondemented cases with AD-related pathology, the authors investigated 47 brains from demented and nondemented patients with AD-related pathology covering all phases of β-amyloidosis in the MTL (AβMTL phases) and four control brains without any AD-related pathology. *Methods:* Aβ deposits were detected by the use of the Campbell-Switzer silver technique and by immunohistochemistry in sections covering all brain regions and brainstem nuclei. It was analyzed how often distinct regions exhibited Aβ deposits. *Results:* In the first of five phases in the evolution of β-amyloidosis Aβ deposits are found exclusively in the neocortex. The second phase is characterized by the additional involvement of allocortical brain regions. In phase 3, diencephalic nuclei, the striatum, and the cholinergic nuclei of the basal forebrain exhibit Aβ deposits as well. Several brainstem nuclei become additionally involved in phase 4. Phase 5, finally, is characterized by cerebellar Aβ-deposition. The 17 clinically proven AD cases exhibit Aβ-phases 3, 4, or 5. The nine nondemented cases with AD-related Aβ pathology show Aβ-phases 1, 2, or 3. *Conclusions:* Aβ-deposition in the entire brain follows a distinct sequence in which the regions are hierarchically involved. Aβ-deposition, thereby, expands anterogradely into regions that receive neuronal projections from regions already exhibiting Aβ. There are also indications that clinically proven AD cases with full-blown β-amyloidosis may be preceded in early stages by nondemented cases exhibiting AD-related Aβ pathology.

NEUROLOGY 2002;58:1791–1800

AD is histopathologically characterized by the presence of cerebral amyloid β protein (Aβ) deposits, neuritic plaques (NP), neurofibrillary tangles (NFT), and neuropil threads (NT).[1-4] The distribution of NFT-bearing neurons and the severity of neurofibrillary pathology allow the distinction of six stages (NFT stages) in the disease propagation[1] correlating with both the degree of Aβ-plaque pathology and the intellectual decline gradually developing during the course of AD.[1,5-10] According to recent observations, Aβ-deposition follows a distinct sequence in which the regions of the medial temporal lobe (MTL) become hierarchically involved.[11]

Outside the MTL, Aβ-deposits are seen in all parts of the allo- and neocortex, in the striatum, the hypothalamus, the thalamus, the basal forebrain nuclei, the cerebellum, and in several brainstem nuclei.[1,12-27] At this point, it is not known whether β-amyloidosis outside the MTL expands in a hierarchical manner as well, whether in clinically proven AD cases it represents a later stage of β-amyloidosis seen in nondemented patients with AD-related neuropathology, or whether β-amyloidosis in AD is substantially different from Aβ-deposition in nondemented individuals.

To provide this information we studied Aβ-deposition in serial sections through the brains of clinically proven AD cases, nondemented cases with AD-related pathology (ADRP), and nondemented controls without ADRP.

Additional material related to this article can be found on the *Neurology* Web site. Go to www.neurology.org and scroll down the Table of Contents for the June 25 issue to find the title link for this article.

Materials and methods. *Neuropathologic assessment.* Brains from 51 autopsy cases from both sexes, aged 42 to 93 years, were investigated (see the table in the online version of this article at www.neurology.org). All cases were free of relevant non-AD-related neuropathologic alterations except for two AβMTL phase 1 cases, one with PD (Case 13) and one with progressive supranuclear palsy–related pathology (Case 14). Neither of the cases showed Aβ-deposition different from the other phase 1 cases and were therefore accepted for demonstrating Aβ pathology, but both were excluded from statistical analysis. The cases had usually been examined 1 to 4 weeks

From the Department of Anatomy (Drs. Thal, Rüb, and Braak), J. W. Goethe University, Frankfurt am Main; Department of Neuropathology (Dr. Thal), University of Bonn Medical Center, Bonn; and Department of Pathology (Dr. Orantes), Municipal Hospital of Offenbach, Offenbach am Main, Germany.

Supported by DFG—grant no. TH 624/4-1 and BONFOR—grant nos. O-154.0041 and O-154.0043.

Received September 24, 2001. Accepted in final form March 12, 2002.

Address correspondence and reprint requests to Dr. D.R. Thal, Institut für Neuropathologie, Universität Bonn, Sigmund Freud Str. 25, D-53105 Bonn, Germany; e-mail: Dietmar.Thal@uni-bonn.de

Copyright © 2002 by AAN Enterprises, Inc.

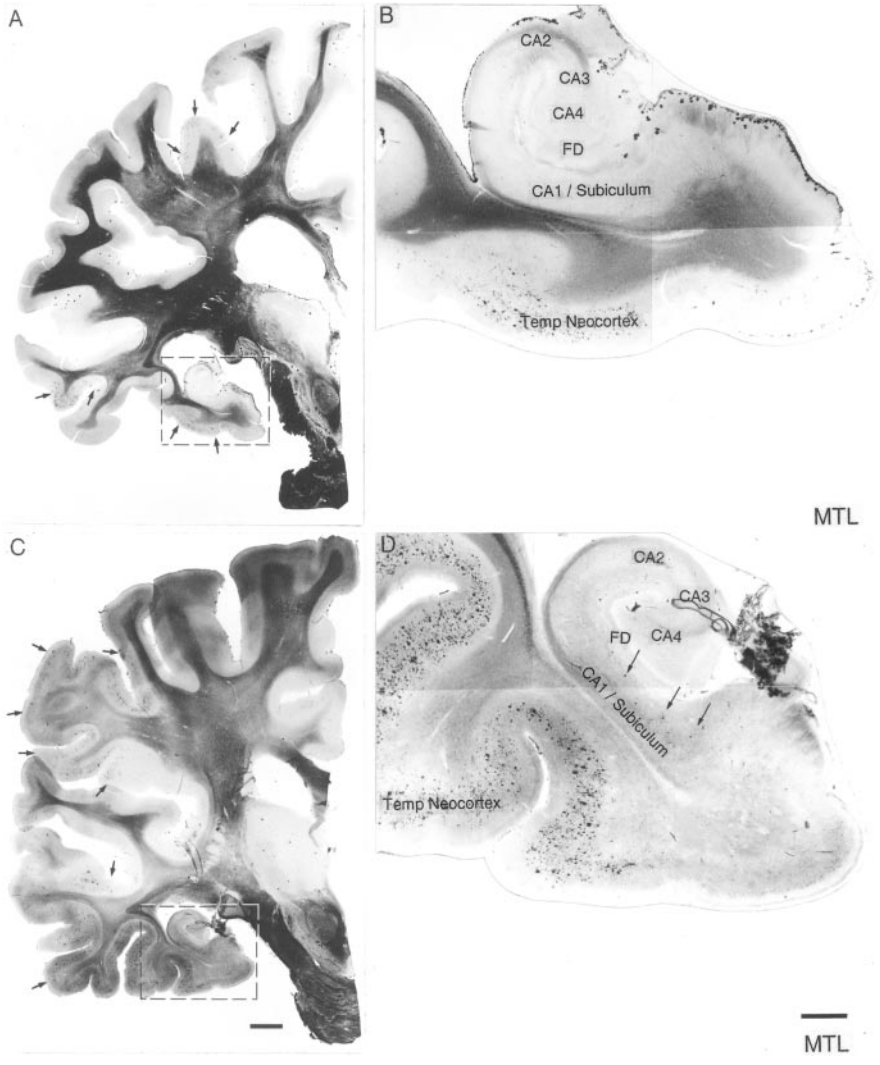

Figure 1. A: Coronal section of an Aβ phase 1 case. This case exhibits Aβ deposits only in the neocortex. There are spots of Aβ deposits in the inferior parietal sulcus, in the superior temporal sulcus, and in the basal temporal neocortex (arrows). B: Note that there are only few diffuse plaques which are restricted to layers II, III, IV, and V as shown in the basal temporal neocortex (B). C: Coronal section of an Aβ phase 2 case. This case shows Aβ deposits in larger areas of the frontal and temporal neocortex (arrows) as well as in CA1. D: The Aβ deposits in CA1 are clearly seen in the higher magnification level (arrows). Note that neocortical Aβ deposits are now found in layers II, III, IV, and V as shown in the basal neocortex. FD = fascia dentata. (Coronal sections; Campbell-Switzer staining; A, B: Case 10; C, D: Case 15; Calibration bar: A, C: 10,000 μm; B, D: 1,666 μm.)

prior to death by different clinicians according to standardized protocols. The protocols included the assessment of cognitive function and recorded the ability to care for and dress oneself, eating habits, bladder and bowel continence, speech patterns, writing and reading, short-term and long-term memory, and orientation within the hospital setting. These data were used to retrospectively assess CDR scores for each patient[28] (see the table in the online version of this article at www.neurology.org). For this purpose, the data from the clinical protocols were transformed into CDR-levels according to the standard CDR-protocol.[28] For Cases 7, 9, 11, 12, 18, 20, 21, 23–26, 28, 30, 32, 36, 38, 42, 44, and 45, sufficient clinical recordings that allowed the determination of CDR scores were not available. AD was diagnosed according to the recently published consensus criteria.[6] Cases with AD-related neurofibrillary or Aβ pathology that were clinically diagnosed as being cognitively normal (CDR = 0) were categorized as putatively nondemented cases with AD-related pathology (ADRP cases). ADRP cases as defined in our study also include Aβ-only and NFT-only cases. The control cases showed no dementia (CDR = 0).

The brains were fixed in a 4% aqueous solution of formaldehyde for at least 3 weeks. After removal of the brainstem and the cerebellum, the right hemisphere of 18 cases was cut coronally into 1 cm thick slices. The brainstem and the cerebellum were cut perpendicular to the Meynert brainstem axis into 5 mm thick slices. One block of the superior frontal gyrus, the superior parietal lobe, areas 17, 18, and 19, the cingulate gyrus, the anterior MTL including the entorhinal region, the middle and posterior MTL with the hippocampus, the basal ganglia, the basal nucleus of Meynert, the septum, the hypothalamus, the thalamus, the midbrain, the pons, the medulla oblongata, and the cerebellum were embedded in paraffin and 10 μm thick sections were cut.

One hemisphere of the other 33 cases (indicated with an asterisk in the table in the online version of this article at www.neurology.org) was cut coronally into an anterior, middle, and posterior block, which were embedded in PEG after dissecting the brainstem at the upper pons level. After removal of the cerebellum the brainstems were embedded in PEG and cut serially perpendicular to the Meynert brainstem axis. One block of the cerebellar cortex and the dentate nucleus from each of these cases were embedded in paraffin. Material from pons and medulla oblongata was not available in Cases 27, 31, and 41. All PEG blocks were cut into serial sections at 100 μm, whereas the paraffin blocks from the cerebellum were microtomed at 10 μm.

Every tenth section of the 33 PEG-embedded hemispheres and 30 brainstems, as well as one paraffin section from each paraffin block, was stained with the Gallyas

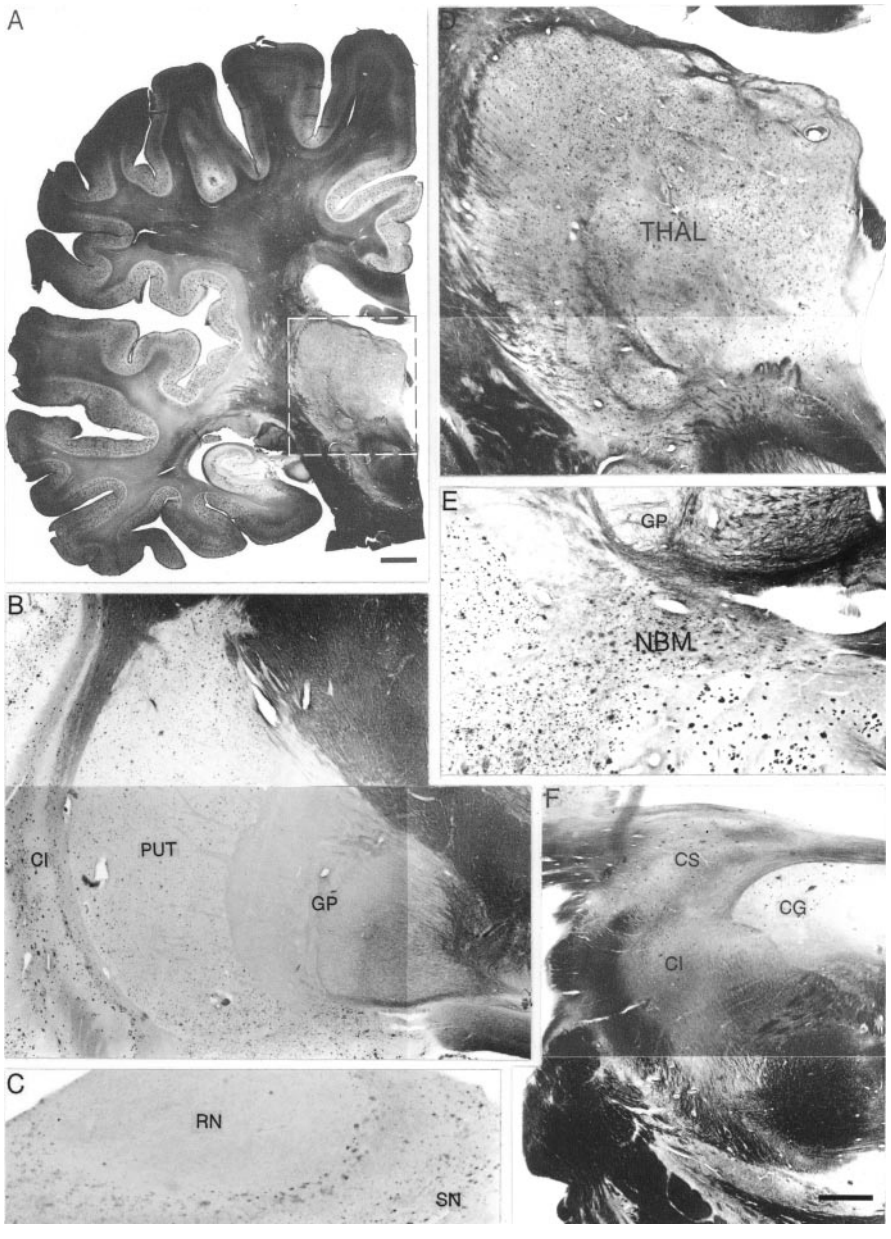

Figure 2. Aβ-deposition in subcortical nuclei in cases of fully developed β-amyloidosis. A, D: The coronal section shows Aβ deposits in all fields of the neocortex, in the entorhinal region, in all subfields of the hippocampal formation, the presubicular region, and in the thalamus (THAL). D: In the thalamus there are Aβ deposits in all subnuclei as shown in higher magnification of the marked area. B, C, E, F: At this phase Aβ deposits occur also in the putamen (PUT) (B), the claustrum (Cl) (B), the basal nucleus of Meynert (NBM) (E), the central gray (CG) (F), the substantia nigra (SN) (C), the red nucleus (RN) (C), and the superior (CS) and inferior collicle (CI) (F). Coronal sections; Campbell-Switzer staining; A, D, E: Case 32 (Aβ phase 4); B, F: Case 40 (Aβ phase 5); C: Case 39 (Aβ phase 5); Calibration bar: A: 10,000 μm; F is valid for B-F: B, D, F: 4,000 μm; C: 330 μm; E: 720 μm.

silver method for detection of NFT, NT, and NP. Likewise, paraffin and PEG sections were stained with the Campbell-Switzer silver method for the detection of amyloid deposits.[29,30] The sensitivity of this technique for the detection of amyloid deposits is equal to that of immunohistochemistry with anti-$A\beta_{17-24}$ (4G8).[11,31]

For purposes of topographic orientation, paraffin and PEG sections were stained with aldehydfuchsin-darrow red for lipofuscin pigment and Nissl material. The distribution of NFT and NT was assessed and diagnosis of stages in the development of neurofibrillary changes (NFT stage) was performed using published criteria and were achieved without knowledge of clinical or pathologic data, age, or sex of the individuals (see the table in the online version of this article at www.neurology.org).[1,6] The phases of β-amyloidosis in the MTL were carried out using Campbell-Switzer stained sections as recently published.[11] The Consortium to Establish a Registry for Alzheimer's Disease (CERAD) neuritic plaque score was determined by estimating the mean neuritic plaque frequency in the hippocampus and in the frontal, parietal, temporal, and occipital cortex as stained with the Gallyas silver method according to published criteria.[6,32]

Immunohistochemistry. In paraffin and PEG sections, the presence of Aβ was observed with an antibody directed against $A\beta_{17-24}$ (4G8, Signet [Dedham, MA], 1/5000, 48 hours at 4 °C) after formic acid pretreatment. The primary antibody was detected with a biotinylated secondary antibody and the ABC complex, and visualized with 3,3-diaminobenzidine (DAB).[33] Immunostained paraffin sections were counterstained with hematoxylin.

Morphologic analysis. The presence of Aβ deposits detectable with the Campbell-Switzer method as well as with anti-Aβ-immunohistochemistry was examined in the hippocampal sectors CA1, CA2, CA3, and CA4, the outer and inner portion of the molecular layer of the fascia dentata, the fascia dentata granule cell layer, the layers of the entorhinal cortex, all neocortical areas, the cingulate gyrus, the basal

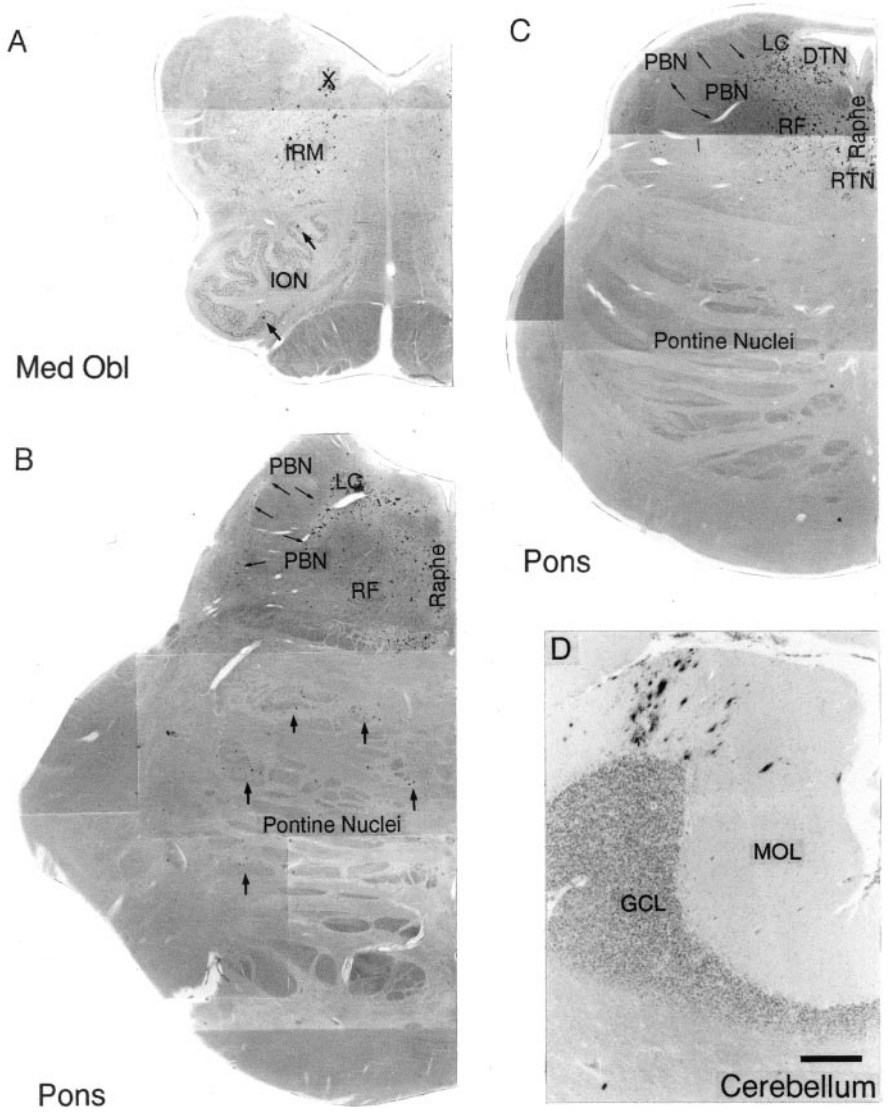

Figure 3. Aβ-deposition in the lower brainstem and in the cerebellum in phase 5 of β-amyloidosis. In this end phase of β-amyloidosis Aβ-deposition takes place in lower brainstem nuclei and the cerebellum. A–C: Aβ deposits occur in the following lower brainstem nuclei: intermediate reticular zone of the medulla oblongata (A [IRM]), the reticular formation of the pons (B, C [RF]), the locus coeruleus (B, C [LC]), the oral and central raphe nuclei (B, C [Raphe]), the parabrachial nuclei (B, C [PBN]), the dorsal tegmental nucleus (C [DTN]), the reticulo-tegmental nucleus (C [RTN]), the pontine nuclei (B, C), and the inferior olivary nucleus (A [ION]). D: In the cerebellum, Aβ deposits are most frequently restricted to the molecular layer (MOL). GCL = cerebellar granule cell layer. Sections perpendicular to the Meynert brainstem axis; Campbell-Switzer staining; Case 39 (A, C); Case 35 (B); Case 32 (D); Calibration bar in D valid for A–D: A, B, C: 4,000 μm, D: 300 μm.

nucleus of Meynert, the hypothalamus, the thalamus, the basal ganglia, the subthalamic nucleus, the midbrain, the pons, the medulla oblongata, and the cerebellum.

For further analysis, it was noted whether Aβ deposits were absent or present in a given region and in how many cases they were present. This was carried out for all of the abovementioned regions. Afterwards, regions with Aβ deposits in a high number of cases were compared with regions exhibiting Aβ deposits in a lesser number of cases to see if cases in the latter category consistently show Aβ deposits in regions of the former category as well. In doing so, we studied whether there is a distinct sequence in which the regions of the brain become involved in β-amyloidosis. In the event that there is evidence for a hierarchical sequence in which brain regions are involved in β-amyloidosis, the phases are generated according to the following criteria: 1) regions involved in early phases are those that exhibit Aβ deposits in the majority of cases, whereas the regions in which only a few cases show Aβ are end-stage cases; 2) brain regions exhibiting Aβ deposits in early AβMTL-phases may represent early affected brain regions and regions involved only in advanced AβMTL-phases may represent late stage Aβ-deposition. Furthermore, we counted the number of regions exhibiting Aβ deposits in each case.

Statistical analysis. The modified χ^2 test according to Cochran[34] was used to determine whether there is a constant sequence in which the brain regions are involved in β-amyloidosis. For investigating whether the number of regions involved in β-amyloidosis in ADRP cases is different from that in AD cases we used the Mann-Whitney *U*-test. Spearman correlation for ranked variables was used to determine whether increasing Aβ-deposition in the whole brain is correlated with the progression of Aβ-deposition in the MTL or with the progression of neurofibrillary pathology as indicated by the NFT stages or with the CDR score.

Results. *Hierarchical sequence of Aβ-deposition.* Eighty-six percent of the cases examined in this study exhibited Aβ deposits in the neocortex. Seventy-two percent of them showed Aβ in the allocortex, 58% of the cases in the striatum, the cholinergic nuclei of the basal forebrain, the hypothalamus, and the thalamus, 48% of the cases in the brainstem, and 35% of the cases in the cerebellum (figures

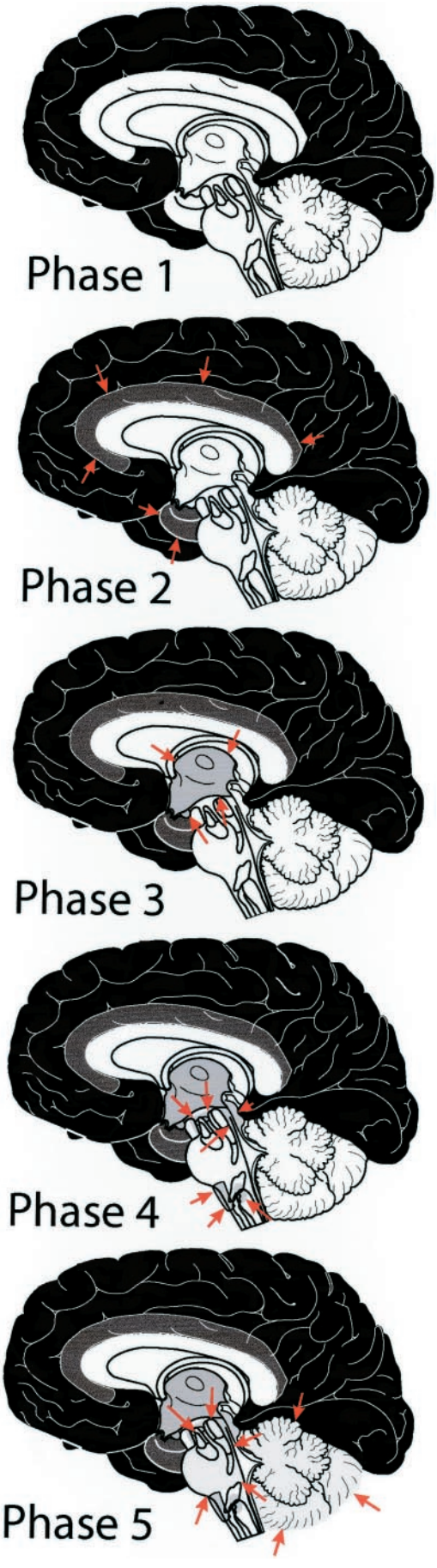

1 through 4, and the table). These local differences in the frequency of the occurrence of Aβ deposits allow identification of five phases of Aβ-deposition in which the brain regions are hierarchically involved.

In phase 1, there are Aβ deposits in the frontal, parietal, temporal, or occipital neocortex. These deposits appear focally in small groups of diffuse plaques in layers II, III, IV, and V. In five of six cases Aβ-deposition is seen in the temporal neocortex, in four cases in the frontal neocortex, in two cases in the parietal neocortex, and in five cases in the occipital neocortex. All other regions of the brain do not exhibit any Aβ deposits (see figure 1, A and B, and the table).

Thereafter, in phase 2, in addition to the neocortical Aβ deposits seen in phase 1, Aβ appears in the entorhinal region, CA1, and in the insular cortex. In 33–50% of the phase 2 cases, single Aβ deposits occur in the amygdala, the cingulate gyrus, the presubicular region, the molecular layer of the fascia dentata, and small patches of subpial band-like amyloid appear in the frontal, parietal, temporal, and occipital neocortex (table). All other areas do not show Aβ in this phase (see figure 1, C and D).

Phase 3 is characterized by the occurrence of Aβ within the following subcortical regions: caudate nucleus, putamen, claustrum, basal forebrain nuclei, substantia innominata, thalamus, hypothalamus (including the mamillary body), lateral habenular nucleus, and white matter. In the presubicular region, lake-like amyloid is now seen. Aβ deposits also appear in the molecular layer of the fascia dentata. Subpial band-like amyloid occurs in the subpial zone in all parts of the neocortex as well as in the entorhinal region and the cingulate gyrus. All the regions exhibiting Aβ deposits in phases 1 and 2 also have them in phase 3. Within the central gray in the midbrain, the colliculi superiores and inferiores, CA4, the red nucleus, and the subthalamic nucleus, Aβ deposits appear in 10–45% of the phase 3 cases (table). All other regions are free of Aβ.

Phase 4 of β-amyloidosis (figure 2, and the table) is characterized by additional Aβ deposits in the inferior olivary nucleus, the reticular formation of the medulla oblongata, and the substantia nigra (see figure 2C, SN). CA4, the central gray of the midbrain (see figure 2F, CG), the colliculi superiores (see figure 2F, CS) and inferiores (see figure 2F, CI), and the red nucleus (see figure 2C, RN) now constantly exhibit Aβ deposits. Within the inferior olivary nucleus, the reticular formation of the pons and the medulla oblongata, and the red nucleus there are often only one to three plaques in the entire anatomic structure.

Figure 4. Phases of β-amyloidosis. Phase 1 is characterized by exclusively neocortical Aβ deposits (Neocortex: black). Phase 2 shows additional allocortical Aβ deposits (red arrows), phase 3 additional Aβ deposits in diencephalic nuclei (red arrows) and the striatum (not shown), phase 4 additional Aβ deposits in distinct brainstem nuclei (substantia nigra, red nucleus, central gray, superior and inferior collicle, inferior olivary nucleus, and intermediate reticular zone) (red arrows), and phase 5 in the cerebellum and additional brainstem nuclei (pontine nuclei, locus coeruleus, parabrachial nuclei, reticulo-tegmental nucleus, dorsal tegmental nucleus, and oral and central raphe nuclei) (red arrows).

Table *Percentage of cases exhibiting Aβ-deposition in a given phase in a given region*

	Aβ Phase 1	Aβ Phase 2	Aβ Phase 3	Aβ Phase 4	Aβ Phase 5
Neocortex	100,00%	100,00%	100,00%	100,00%	100,00%
CA1	0,00%	100,00%	100,00%	100,00%	100,00%
Entorhinal Region	0,00%	83,30%	100,00%	100,00%	100,00%
Gyrus cinguli	0,00%	50,00%	88,90%	100,00%	100,00%
Amygdala	0,00%	33,30%	88,90%	100,00%	100,00%
Fascia Dentata	0,00%	33,30%	77,80%	100,00%	100,00%
Presubiculum	0,00%	33,30%	100,00%	100,00%	100,00%
Thalamus	0,00%	0,00%	88,90%	100,00%	100,00%
Striatum	0,00%	0,00%	77,80%	100,00%	100,00%
Hypothalamus	0,00%	0,00%	77,80%	100,00%	100,00%
Basal Forebrain Nuclei (Meynert)	0,00%	0,00%	55,60%	100,00%	100,00%
CA4	0,00%	16,70%	22,20%	100,00%	100,00%
Central Gray	0,00%	0,00%	44,40%	80,00%	100,00%
Superior Collicle	0,00%	0,00%	44,40%	80,00%	88,90%
Red Nucleus	0,00%	0,00%	11,10%	80,00%	88,90%
Inferior Olivary Nucleus	0,00%	0,00%	0,00%	75,00%	100,00%
Substantia Nigra	0,00%	0,00%	0,00%	60,00%	66,70%
Reticular Formation of the Medulla Oblongata	0,00%	0,00%	0,00%	50,00%	75,00%
Cerebellar Molecular Layer	0,00%	0,00%	0,00%	0,00%	100,00%
Reticular Formation of the Pons	0,00%	0,00%	0,00%	0,00%	75,00%
Anterior and Central Raphe nuclei	0,00%	0,00%	0,00%	0,00%	62,50%
Locus coeruleus	0,00%	0,00%	0,00%	0,00%	62,50%
Parabrachial Nuclei	0,00%	0,00%	0,00%	0,00%	62,50%
Reticulo Tegmental Nucleus (Bechterew)	0,00%	0,00%	0,00%	0,00%	62,50%
Dorsal Tegmental Nucleus (Gudden)	0,00%	0,00%	0,00%	0,00%	62,50%
Nuclei Pontis	0,00%	0,00%	0,00%	0,00%	11,11%
Cerebellar Granule Cell Layer	0,00%	0,00%	0,00%	0,00%	11,11%
Dentate Nucleus	0,00%	0,00%	0,00%	0,00%	0,00%

76%-100%
51%-75%
26%-50%
1%-25%
0%

Regions exhibiting Aβ deposits in phase 1 are marked in black, those in phase 2 in 80% gray, those in phase 3 in 60% gray, those in phase 4 in 40% gray, and those in phase 5 in 20% gray. Regions in white do not show any Aβ deposits.

These plaques are easy to detect in serial brainstem sections, but may escape recognition in every case when studying representative sections alone. All of the brain regions containing Aβ deposits in phases 1–3 also have them in Aβ phase 4. Other brainstem nuclei and the cerebellum do not show Aβ deposits.

In phase 5 of β-amyloidosis (figure 3, and the table), Aβ deposits occur, in addition to those seen already in phase 4, in the reticular formation of the pons (see figure 3C, RF), the pontine nuclei (see figure 3), the central and dorsal raphe nuclei (see figure 3C), the locus coeruleus (see figure 3B, LC), the parabrachial nuclei (see figure 3B, PBN), the dorsal tegmental nucleus (Gudden) (see figure 3C, DTN), the reticulotegmental nucleus of the pons (Bechterew) (see figure 3B, RTN), and the cerebellum (see figure 3D). In the cerebellum, Aβ most frequently occurs in the molecular layer (see figure 3D, MOL). In one case, Aβ is also seen in the cerebellar granular layer, but none of our cases exhibit Aβ in the dentate nucleus or other cerebellar nuclei.

Expansion of Aβ and NFT pathology in AD and ADRP cases. Nondemented cases with ADRP exhibit either neurofibrillary tangles without Aβ or Aβ deposits during Aβ phases 1–3 (figure 5A). NFT stages of the ADRP cases range between 0 and III. AD cases exhibit Aβ phases 3–5. NFT-stages in AD cases range between III and VI (see figure 5A and the table in the online version of this article at www.neurology.org). The four cases diagnosed as nondemented control cases do not exhibit Aβ deposits or neurofibrillary changes (see figure 5A).

All 13 cases with a CDR score of 0 correspond to Aβ phases 0 to 3 and NFT stages 0 to III. The mild AD case with CDR 0.5 shows Aβ phase 5 and NFT stage V. The second CDR 0.5 case exhibits progressive supranuclear palsy–related pathology and is not used for this clinicopathologic correlation. The two CDR 1 cases represent Aβ phases 4 and 5 and NFT stages V and VI. Three cases show a CDR score of 2, and demonstrated Aβ phases 3 and 5 and NFT stages III and IV. The 11 CDR 3 cases exhibit Aβ phases 4 and 5 and NFT stages III-VI (see figure 5B).

Statistical analysis. The neocortex is involved in β-amyloidosis earlier than the allocortical regions (entorhinal region, hippocampus) (χ^2-test in the modification according to Cochran,[34] $p < 0.0001$), which in turn show Aβ deposits before the striatum and the thalamus (χ^2-test in the modification according to Cochran,[34] $p < 0.0001$). The striatum and the thalamus are involved in β-amyloidosis before brainstem regions such as the central gray and the colliculi superior and inferior are involved (χ^2-test in the modification according to Cochran,[34] $p < 0.0001$), and these brainstem regions exhibit Aβ before it is seen in the cerebellum (χ^2-test in the modification according to Cochran,[34] $p < 0.0001$). As such, we show that the sequence in which the regions of the brain are involved in β-amyloidosis is statistically significant.

Correlation analysis reveals a correlation between Aβ phase and AβMTL phase (Spearman's rank correlation coefficient: $r = 0.936$, $p < 0.001$) and between Aβ phase and NFT stage (Spearman's rank correlation coefficient: $r = 0.844$, $p < 0.001$). The CDR score correlates with the Aβ phase (Spearman's rank correlation coefficient: $r = 0.885$, $p < 0.001$), the AβMTL phase (Spearman's rank correlation coefficient: $r = 0.896$, $p < 0.001$), the CERAD neuritic plaque score (Spearman's rank correlation coefficient: r =

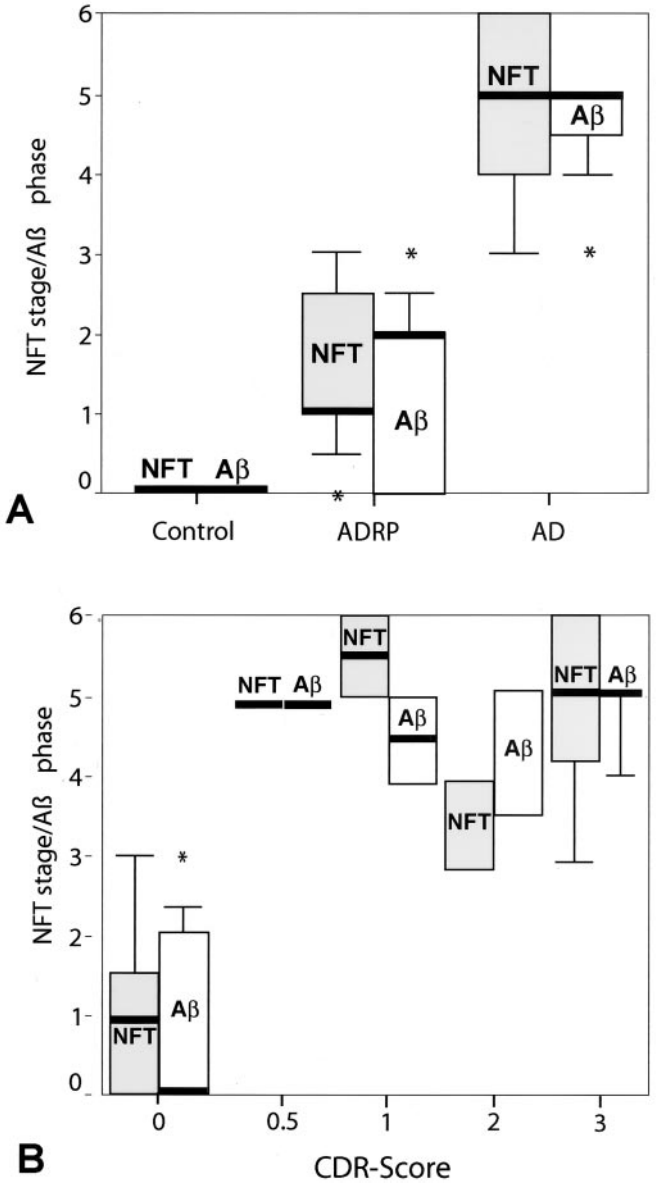

Figure 5. A: Boxplot of NFT stage (NFT) and Aβ phase (Aβ) of control cases, ADRP cases, and clinically proven AD cases. The nondemented ADRP cases show a lower state of expansion of Aβ-deposition and neurofibrillary pathology than demented AD cases as indicated by both the Aβ phase and the NFT stage (Mann-Whitney U*-test:* $p < 0.0001$*). B: Boxplot of NFT stage and Aβ phase of cases with CDR scores 0, 0.5, 1, 2, and 3. The nondemented CDR 0 cases show a lower state of expansion of Aβ-deposition and neurofibrillary pathology than CDR 0.5–3 cases as indicated by both the Aβ phase and the NFT stage. Because only single cases with CDR scores 0.5, 1, and 2 are included in this study, the mean values shown in this boxplot are not representative among cases with these CDR scores. The conclusion drawn from the 13 nondemented CDR 0 cases and 11 demented CDR 3 cases is that in general, an increase in the Aβ phase and NFT stage is related with clinically proven dementia. Whether cases with mild cognitive impairment (CDR 0.5) can be distinguished from nondemented cases and from CDR 3 cases cannot be answered in this study. The boxes contain 50% of the cases, the black bar within the boxes displays the mean, the ranges cover all cases except for single extreme values. These extreme values are indicated with an asterisk. (NFT stage = Stage in the evolution of neurofibrillary pathology according to Braak and Braak[1]; control = nondemented cases without AD-related pathology; ADRP = cases with AD-related pathology and no dementia [CDR = 0]; AD = cases with clinically proven dementia and AD-related pathology.[6])*

0.908, $p < 0.001$), and with the NFT stage (Spearman's rank correlation coefficient: $r = 0.825$, $p < 0.001$).

The Mann-Whitney *U*-test showed that the number of regions exhibiting Aβ deposits as well as the Aβ phase and the NFT stage is higher in AD cases than in ADRP cases ($p < 0.0001$).

Discussion. The evolution of Aβ-deposition in the brain allows the distinction of five phases (figure 4, and the table). The first phase displays only neocortical Aβ deposits. The second phase is characterized by the additional involvement of allocortical brain regions. In phase 3, diencephalic nuclei, the putamen, the caudate nucleus, the substantia innominata, and the magnocellular cholinergic nuclei of the basal forebrain exhibit Aβ deposits as well, whereas several brainstem nuclei first become involved in phase 4. The fifth and final phase is characterized by Aβ-deposition in the cerebellum and in additional brainstem nuclei. The five phases of β-amyloidosis give a more precise description of the evolution of β-amyloidosis in the entire brain than the AβMTL phases[11] and the ABC stages[1] insofar as the hierarchical development of Aβ-deposition in the brainstem and the cerebellum has now been included in describing the expansion of Aβ pathology in the brain.

This sequence in which the regions of the brain are involved in β-amyloidosis shows that Aβ-deposition in the entire brain is a successive process[11] based on the following four arguments: 1) in every case exhibiting a given phase of β-amyloidosis, regions that had Aβ deposits in an earlier phase still contain them at that point; 2) the phases of β-amyloidosis correlate significantly with the evolution of neurofibrillary lesions as documented statistically in the present study; 3) β-amyloidosis in patients with Down's syndrome commences at a young age with a few Aβ deposits in the basal temporal neocortex and successively culminates with the picture of full blown β-amyloidosis at a more advanced age[35,36]; and 4) the recent finding that Aβ-deposition in transgenic mice begins with neocortical Aβ deposits in younger animals followed by Aβ-deposition in other brain regions in older animals[37,38] also favors the theory that this sequential involvement of brain regions is a successive one.

Because the expansion of Aβ throughout the evolution of β-amyloidosis follows a distinct sequence in which the regions of the entire brain are hierarchically involved, the question arises as to why brain regions are involved in this particular sequence or why

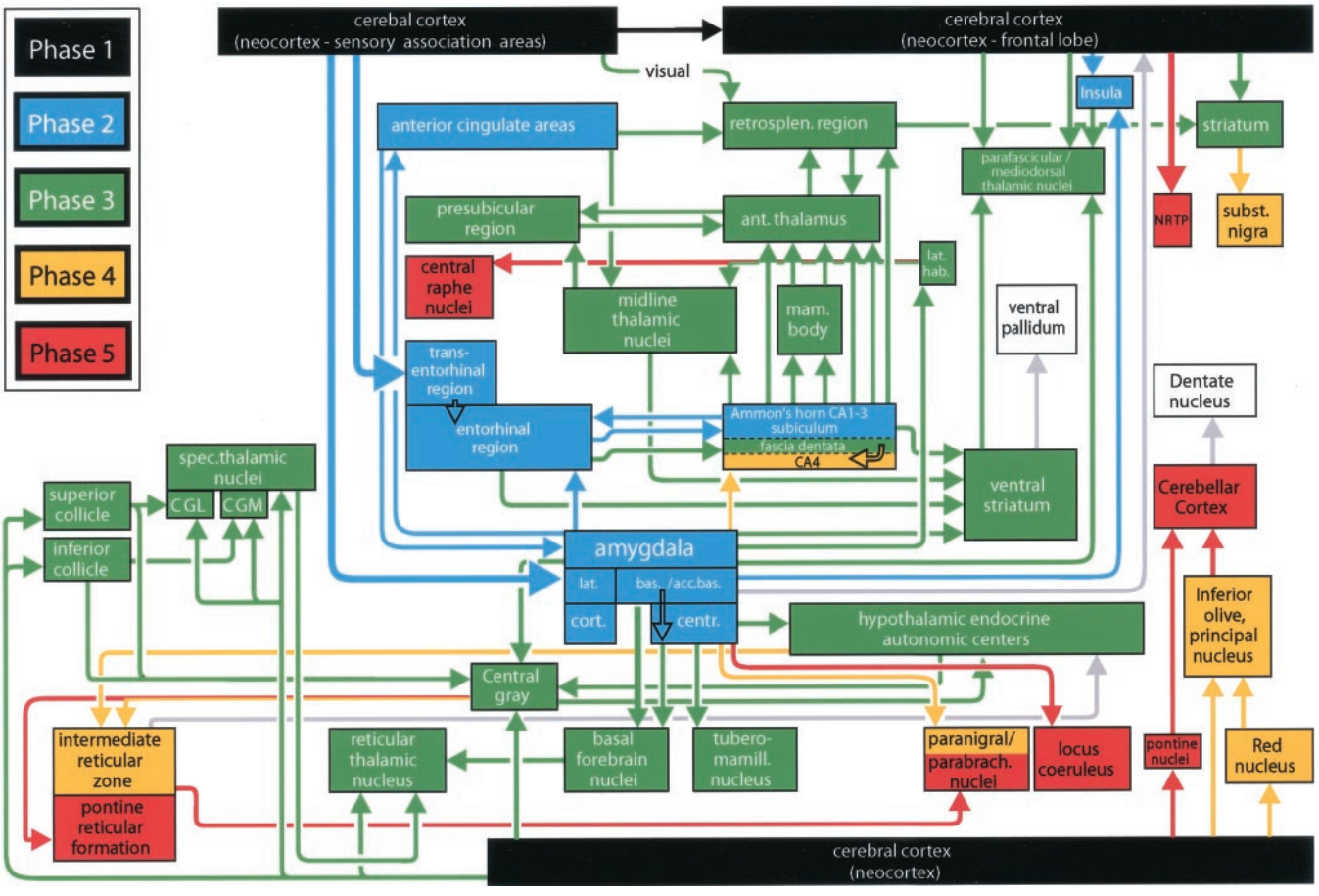

Figure 6. Anterograde expansion of Aβ-deposition: Schematic representation of the brain regions that develop Aβ deposits by way of their direct neuronal connections with each other. The boxes represent a cortical area or a subcortical nucleus. Arrows directed toward the box represent afferent fibers from other brain regions which have synaptic contact with a given cortical area or subcortical nucleus. Arrows pointing away from a given box and directed toward another box represent the efferent fibers of the neurons of a given region which have their targets in the region to which the arrow points. CGL = lateral geniculate body; CGM = medial geniculate body; lat. hab. = lateral habenular nucleus; NRTP = reticulotegmental nucleus of the pons. The NRTP projects to the nucleus fastiguus of the cerebellum and the pontine reticular formation projects to thalamic and hypothalamic nuclei. The colored boxes indicate brain regions with Aβ deposits. The color scale at the left shows the colors that represent phases 1–5 of β-amyloidosis. The colored arrows point to regions becoming involved in a given phase as displayed by the color of the box. If the connection is not relevant for the expansion of β-amyloidosis, it is either not shown or appears in gray. In doing so, connections which are relevant for the expansion of Aβ-deposition are demonstrated for every brain region involved in β-amyloidosis. It becomes evident that, in our cases, all regions involved in β-amyloidosis in phases 2, 3, 4, and 5 receive input from previously affected regions. The neocortical areas that exhibit Aβ deposits in phase 1 (marked in black) project into regions that show Aβ in phase 2 (marked in blue): namely, into the insular cortex,[39] the amygdala,[39] and the transentorhinal region.[39] The entorhinal cortex, also affected in phase 2, receives input from the transentorhinal region[39,40]; CA1 and the subiculum both receive input from the entorhinal cortex[40,41] and both exhibit Aβ deposits only in the event that the entorhinal region also has Aβ deposits. In a similar way, the cingulate gyrus exhibits Aβ in the event that the amygdala or the retrosplenial region show Aβ deposits as well. The cingulate gyrus receives input from the amygdala, the retrosplenial region, and the midline thalamic nuclei.[39] The locations in which Aβ appears in phase 3 (marked in green) similarly receive afferent input from regions that exhibit Aβ in phases 1 and 2, namely: 1) the presubiculum receives input from the distal subiculum and the midline thalamic nuclei,[40] which become involved in β-amyloidosis in phase 3 as well, 2) the fascia dentata receives input from the entorhinal cortex,[40] 3) the thalamic nuclei acquire input from the neocortex and the hippocampus,[39] 4) the hypothalamic nuclei obtain input from the amygdala and the hippocampus,[39] 5) the striatum receives input from the neocortex, cingulate cortex, and parabrachial nuclei,[39] 6) the basal forebrain acquires input from the amygdala,[39] 7) the central gray receives input from the amygdala, the hypothalamus, and the neocortex,[39,42] and 8) the superior and inferior colliculus[43] receive, among others, input from the cerebral cortex.[44] In phase 4, Aβ appears in the pre-α layer of the entorhinal cortex, CA4, the red nucleus, the inferior olivary nucleus, the substantia nigra, and the reticular formation of the medulla oblongata, which all receive afferent input from previously affected regions either from the neocortex[39,45] or from central gray neurons that project into the reticular formation of the medulla oblongata (marked in yellow).[43] Finally, in the fifth phase the newly affected regions (marked in red) receive input from regions already exhibiting Aβ deposits: 1) the molecular layer of the cerebellar cortex receives afferent fibers from the inferior olivary nucleus,[45] 2) the parabrachial nuclei receive

they do not occur by chance. The neocortex is always the first region to develop Aβ deposits. Thus, it is tempting to speculate that this region has the highest susceptibility for the deposition of Aβ. Afterwards, all regions becoming involved in β-amyloidosis in phases 2, 3, 4, and 5 receive afferent input from previously or simultaneously affected regions as shown in detail in figure 6. In so doing, Aβ-deposition in the entire brain expands in an anterograde direction from regions already exhibiting Aβ deposits into regions that receive neuronal input from these regions. Because different brain regions (e.g., the amygdala and the pontine nuclei) all receive input from one Aβ-containing region (e.g., the neocortex [see figure 6]) but become involved in β-amyloidosis at different phases (e.g., the amygdala in Aβ phase 2 and the pontine nuclei in Aβ phase 5), one is inclined to conclude that regional susceptibility for Aβ-deposition plays an additional role in determining when a given region becomes involved in β-amyloidosis.

Furthermore, in our small sample we could show that 17 clinically proven AD cases exhibited Aβ phases 3, 4, and 5 and NFT stages III–VI whereas the nine nondemented cases with ADRP showed Aβ phases 0, 1, 2, and 3 and NFT stages 0–III. Because we have shown that Aβ-deposition in the brain is a process beginning with neocortical Aβ-deposition in Aβ phase 1, then expanding step by step into further regions of the brain, culminating with full-blown β-amyloidosis in Aβ phase 5, our results indicate that fully developed β-amyloidosis (Aβ phases 4 and 5) in AD is the final result of a process starting with neocortical Aβ deposits (Aβ phase 1) in nondemented individuals. The same applies for development of neurofibrillary pathology, which begins in the transentorhinal region in nondemented individuals and then expands, ending in full-blown neurofibrillary pathology in a large number of brain regions in AD cases.[1] Because early stages of AD-related Aβ or neurofibrillary pathology, including Aβ-only and NFT-only cases, appear to be early steps in the process leading finally to the pathologic picture of AD, it is tempting to speculate that nondemented cases exhibiting early stages of AD-related pathology represent preclinical stages of AD. In doing so, it is important to subdivide nondemented aged cases (cases of "normal aging") into ADRP cases presumably representing preclinical stages of AD and control cases without any signs of neurodegeneration. Whether "preclinical" AD cases will inevitably develop AD cannot be answered so far.

Although demented individuals show higher Aβ phases than nondemented individuals, it is still questionable whether there is a correlation between an increasing degree of dementia and Aβ phases. In our sample, only single cases exhibit CDR scores of 0.5, 1, and 2, so we cannot answer this question at the moment. A recent study, however, indicates that the phases of β-amyloidosis in the MTL correlate with the degree of dementia.[49] Because the phases of β-amyloidosis in the MTL correspond in most cases to the Aβ phases it is tempting to speculate that Aβ phases correlate likewise.

From a clinical point of view, our findings about the Aβ phases suggest that AD is a disease in which large areas of the brain develop pathologic Aβ deposits (Aβ phases 1 to 3) before clinical symptoms become apparent and that clinically proven AD is a late stage of this process starting much earlier in nondemented individuals. Therefore, one could hypothesize that treatment of AD is more successful the earlier the expansion of Aβ and NFT pathology is stopped, at best in preclinical cases. As soon as imaging techniques, as described for the detection of Aβ in transgenic mice,[50,51] allow the detection of Aβ in the human brain in vivo, Aβ phases could be determined in patients and would make it possible 1) to recognize preclinical phases of AD and 2) to determine the phase of AD in demented patients. This could help in choosing the best therapeutic strategy for the individual patient in the future.

Acknowledgment

The authors thank A. Biczysko, R. Schneider, U. Gruner, A. Börner, U. Fertig, M. Walter, M. Babl, M. Lazar, Mr. H. Friedrich, T. Chatsopoulos, R. Baldauf, I. Szasz, U. Klatt, and S. Janik for technical assistance; Mrs. K. Gierga and Dr. K. Del Tredici for editing the manuscript; and Dr. P. Müller for providing autopsy material.

References

1. Braak H, Braak E. Neuropathological stageing of Alzheimer-related changes. Acta Neuropathol (Berl) 1991;82:239–259.
2. Dickson DW. The pathogenesis of senile plaques. J Neuropathol Exp Neurol 1997;56:321–339.
3. Esiri MM, Hyman BT, Beyreuther K, Masters CL. Ageing and dementia. In: Graham DI, Lantos PL, eds. Greenfields neuropathology, Vol. 2. London: Arnold, 1996:153–233.
4. Masters CL, Simms G, Weinman NA, Multhaup G, McDonald BL, Beyreuther K. Amyloid plaque core protein in Alzheimer disease and Down syndrome. Proc Natl Acad Sci USA 1985;82:4245–4249.
5. Bancher C, Braak H, Fischer P, Jellinger KA. Neuropathological staging of Alzheimer lesions and intellectual status in Alzheimer's and Parkinson's disease patients. Neurosci Lett 1993;162:179–182.
6. The National Institute on Aging, and Reagan Institute Working Group on Diagnostic Criteria for the Neuropathological Assessment of Alzheimer's Disease. Consensus recommendations for the postmortem diagnosis of Alzheimer's disease. The National Institute on Aging, and Reagan Institute Working Group on Diagnostic Criteria for the Neuropathological As-

input from the amygdala,[39,42] 3) the central and dorsal raphe nuclei receive input from the habenular nucleus of the thalamus,[39,42] 4) the pontine nuclei acquire input from the neocortex,[39,42] 5) the reticular formation of the pons receives input from the central gray,[39,42] 6) the dorsal tegmental nucleus (Gudden) obtains afferent fibers from the lateral habenular nucleus of the thalamus,[39,43,46] 7) the reticulo-tegmental nucleus of the pons acquires input from the frontal cortex,[47,48] and 8) the granule cell layer of the cerebellar cortex receives input from the pontine nuclei.

sessment of Alzheimer's Disease. Neurobiol Aging 1997;18(4 suppl):S1–S2.
7. Cummings BJ, Cotman CW. Image analysis of beta-amyloid load in Alzheimer's disease and relation to dementia severity. Lancet 1995;346:1524–1528.
8. Naslund J, Haroutunian V, Mohs R, et al. Correlation between elevated levels of amyloid beta-peptide in the brain and cognitive decline. JAMA 2000;283:1571–1577.
9. Thal DR, Arendt T, Waldmann G, et al. Progression of neurofibrillary changes and PHF-tau in end-stage Alzheimer's disease is different from plaque and cortical microglial pathology. Neurobiol Aging 1998;19:517–525.
10. Thal DR, Holzer M, Rüb U, et al. Alzheimer-related tau-pathology in the perforant path target zone and in the hippocampal stratum oriens and radiatum correlates with onset and degree of dementia. Exp Neurol 2000;163:98–110.
11. Thal DR, Rüb U, Schultz C, et al. Sequence of Abeta-protein deposition in the human medial temporal lobe. J Neuropathol Exp Neurol 2000;59:733–748.
12. Duyckaerts C, Hauw JJ, Bastenaire F, et al. Laminar distribution of neocortical senile plaques in senile dementia of the Alzheimer type. Acta Neuropathol (Berl) 1986;70:249–256.
13. Gearing M, Schneider JA, Robbins RS, et al. Regional variation in the distribution of apolipoprotein E and A beta in Alzheimer's disease. J Neuropathol Exp Neurol 1995;54:833–841.
14. Braak H, Braak E, Bohl J, Lang W. Alzheimer's disease: amyloid plaques in the cerebellum. J Neurol Sci 1989;93:277–287.
15. Braak H, Braak E, Kalus P. Alzheimer's disease: areal and laminar pathology in the occipital isocortex. Acta Neuropathol (Berl) 1989;77:494–506.
16. Braak H, Braak E. Alzheimer's disease: striatal amyloid deposits and neurofibrillary changes. J Neuropathol Exp Neurol 1990;49:215–224.
17. van de Nes JA, Kamphorst W, Ravid R, Swaab DF. Comparison of beta-protein/A4 deposits and Alz-50-stained cytoskeletal changes in the hypothalamus and adjoining areas of Alzheimer's disease patients: amorphic plaques and cytoskeletal changes occur independently. Acta Neuropathol (Berl) 1998;96:129–138.
18. Braak H, Braak E. Alzheimer's disease affects limbic nuclei of the thalamus. Acta Neuropathol (Berl) 1991;81:261–268.
19. Arendt T, Taubert G, Bigl V, Arendt A. Amyloid deposition in the nucleus basalis of Meynert complex: a topographic marker for degenerating cell clusters in Alzheimer's disease. Acta Neuropathol (Berl) 1988;75:226–232.
20. Mann DM, Jones D, Prinja D, Purkiss MS. The prevalence of amyloid (A4) protein deposits within the cerebral and cerebellar cortex in Down's syndrome and Alzheimer's disease. Acta Neuropathol (Berl) 1990;80:318–327.
21. Iseki E, Matsushita M, Kosaka K, Kondo H, Ishii T, Amano N. Distribution and morphology of brain stem plaques in Alzheimer's disease. Acta Neuropathol (Berl) 1989;78:131–136.
22. Arriagada PV, Marzloff K, Hyman BT. Distribution of Alzheimer-type pathologic changes in nondemented elderly individuals matches the pattern in Alzheimer's disease. Neurology 1992;42:1681–1688.
23. Price JL, Davis PB, Morris JC, White DL. The distribution of tangles, plaques and related immunohistochemical markers in healthy aging and Alzheimer's disease. Neurobiol Aging 1991; 12:295–312.
24. Yamada M, Mehraein P. Distribution of senile changes in brain stem nuclei [in Japanese]. Folia Psychiatr Neurol Jpn 1977;31:219–224.
25. Ogomori K, Kitamoto T, Tateishi J, Sato Y, Suetsugu M, Abe M. Beta-protein amyloid is widely distributed in the central nervous system of patients with Alzheimer's disease. Am J Pathol 1989;134:243–251.
26. Parvizi J, Van Hoesen GW, Damasio A. The selective vulnerability of brainstem nuclei to Alzheimer's disease. Ann Neurol 2001;49:53–66.
27. Scinto LF, Wu CK, Firla KM, Daffner KR, Saroff D, Geula C. Focal pathology in the Edinger-Westphal nucleus explains pupillary hypersensitivity in Alzheimer's disease. Acta Neuropathol (Berl) 1999;97:557–564.
28. Hughes CP, Berg L, Danziger WL, Coben LA, Martin RL. A new clinical scale for the staging of dementia. Br J Psychiatry 1982;140:566–572.
29. Braak H, Braak E. Demonstration of amyloid deposits and neurofibrillary changes in whole brain sections. Brain Pathol 1991;1:213–216.
30. Iqbal K, Braak H, Braak E, Grundke-Iqbal I. Silver labeling of Alzheimer neurofibrillary changes and brain β-amyloid. J Histotechnol 1993;16:335–342.
31. Thal DR, Sassin I, Schultz C, Haass C, Braak E, Braak H. Fleecy amyloid deposits in the internal layers of the human entorhinal cortex are comprised of N-terminal truncated fragments of Abeta. J Neuropathol Exp Neurol 1999;58:210–216.
32. Mirra SS, Heyman A, McKeel D, et al. The consortium to establish a registry for Alzheimer's disease (CERAD). Part II. Standardization of the neuropathologic assessment of Alzheimer's disease. Neurology 1991;41:479–486.
33. Hsu SM, Raine L, Fanger H. Use of avidin-biotin-peroxidase complex (ABC) in immunoperoxidase techniques: a comparison between ABC and unlabeled antibody (PAP) procedures. J Histochem Cytochem 1981;29:577–580.
34. Cochran WG. Some methods for strengthening the common $\chi 2$-test. Biometrics 1954;10:417–451.
35. Lemere CA, Blusztajn JK, Yamaguchi H, Wisniewski T, Saido TC, Selkoe DJ. Sequence of deposition of heterogeneous amyloid beta-peptides and APO E in Down syndrome: implications for initial events in amyloid plaque formation. Neurobiol Dis 1996;3:16–32.
36. Leverenz JB, Raskind MA. Early amyloid deposition in the medial temporal lobe of young Down syndrome patients: a regional quantitative analysis. Exp Neurol 1998;150:296–304.
37. McGowan E, Sanders S, Iwatsubo T, et al. Amyloid phenotype characterization of transgenic mice overexpressing both mutant amyloid precursor protein and mutant presenilin 1 transgenes. Neurobiol Dis 1999;6:231–244.
38. Irizarry MC, Soriano F, McNamara M, et al. Abeta deposition is associated with neuropil changes, but not with overt neuronal loss in the human amyloid precursor protein V717F (PDAPP) transgenic mouse. J Neurosci 1997;17:7053–7059.
39. Braak H, Braak E, Yilmazer D, de Vos RA, Jansen EN, Bohl J. Pattern of brain destruction in Parkinson's and Alzheimer's diseases. J Neural Transm 1996;103:455–490.
40. Witter MP. Organization of the entorhinal-hippocampal system: a review of current anatomical data. Hippocampus 1993; 3(Spec No):33–44.
41. Jones RS. Entorhinal-hippocampal connections: a speculative view of their function. Trends Neurosci 1993;16:58–64.
42. Paxinos G. The human nervous system. San Diego: Academic Press, 1990.
43. Beitz AJ. Central gray. In: Paxinos G, ed. The human nervous system. San Diego: Academic Press, 1990;307–320.
44. Webster WR, Garey LJ. Auditory system. In: Paxinos G, ed. The human nervous system. San Diego: Academic Press, 1990;889–944.
45. Cotman CW, Monaghan DT, Ottersen OP, Storm-Mathisen J. Anatomical organization of excitatory amino acid receptors and their pathways. Trends Neurosci 1987;10:273–280.
46. Hayakawa T, Zyo K. Afferent connections of Gudden's tegmental nuclei in the rabbit. J Comp Neurol 1985;235:169–181.
47. Leichnetz GR, Carlton SM, Katayama Y, et al. Afferent and efferent connections of the cholinoceptive medial pontine reticular formation (region of the ventral tegmental nucleus) in the cat. Brain Res Bull 1989;22:665–688.
48. Gonzalo-Ruiz A, Leichnetz GR, Smith DJ. Origin of cerebellar projections to the region of the oculomotor complex, medial pontine reticular formation, and superior colliculus in New World monkeys: a retrograde horseradish peroxidase study. J Comp Neurol 1988;268:508–526.
49. Gold G, Kovari E, Corte G, Herrmann FR, Canuto A, Bussiere T, Hof PR, Bouras C, Giannakopoulos P. Clinical validity of A beta-protein deposition staging in brain aging and Alzheimer disease. J Neuropathol Exp Neurol 2001;60:946–952.
50. Skovronsky DM, Zhang B, Kung M-P, Kung HF, Trojanowski JQ, Lee V M-Y In vivo detection of amyloid plaques in a mouse model of Alzheimer's disease. Proc Natl Acad Sci USA 2000;97:7609–7614.
51. Wengenack TM, Curran GL, Poduslo JF. Targeting Alzheimer amyloid plaques in vivo. Nat Biotech 2000;1:868–872.